11-27-2015

Observation of B0→p¯ΛD(*)−

Y. Y. Chang et al

Belle Preprint 2015-13
KEK Preprint 2015-22

Observation of $B^0 \to p\bar{\Lambda}D^{(*)-}$

Y.-Y. Chang,[49,*] M.-Z. Wang,[49,†] A. Abdesselam,[62] I. Adachi,[16,12] K. Adamczyk,[50] H. Aihara,[69] S. Al Said,[62,30] D. M. Asner,[54] H. Atmacan,[41] T. Aushev,[43,24] V. Babu,[63] I. Badhrees,[62,29] A. M. Bakich,[61] E. Barberio,[40] B. Bhuyan,[18] J. Biswal,[25] A. Bobrov,[4,52] A. Bozek,[50] M. Bračko,[38,25] T. E. Browder,[15] D. Červenkov,[5] V. Chekelian,[39] A. Chen,[47] B. G. Cheon,[14] K. Chilikin,[24] R. Chistov,[24] V. Chobanova,[39] S.-K. Choi,[13] Y. Choi,[60] D. Cinabro,[75] J. Dalseno,[39,64] M. Danilov,[24,42] J. Dingfelder,[3] Z. Doležal,[5] Z. Drásal,[5] D. Dutta,[63] S. Eidelman,[4,52] H. Farhat,[75] J. E. Fast,[54] T. Ferber,[8] B. G. Fulsom,[54] V. Gaur,[63] N. Gabyshev,[4,52] S. Ganguly,[75] A. Garmash,[4,52] R. Gillard,[75] R. Glattauer,[22] Y. M. Goh,[14] P. Goldenzweig,[27] D. Greenwald,[65] O. Grzymkowska,[50] J. Haba,[16,12] K. Hayasaka,[45] H. Hayashii,[46] X. H. He,[55] W.-S. Hou,[49] C.-L. Hsu,[40] T. Iijima,[45,44] K. Inami,[44] A. Ishikawa,[67] R. Itoh,[16,12] Y. Iwasaki,[16] W. W. Jacobs,[20] I. Jaegle,[15] D. Joffe,[28] K. K. Joo,[6] T. Kawasaki,[51] D. Y. Kim,[59] H. J. Kim,[33] J. B. Kim,[32] J. H. Kim,[31] K. T. Kim,[32] M. J. Kim,[33] S. H. Kim,[14] Y. J. Kim,[31] K. Kinoshita,[7] S. Korpar,[38,25] P. Križan,[35,25] P. Krokovny,[4,52] T. Kuhr,[36] T. Kumita,[71] A. Kuzmin,[4,52] Y.-J. Kwon,[77] Y.-T. Lai,[49] I. S. Lee,[14] L. Li,[57] Y. Li,[74] J. Libby,[19] D. Liventsev,[74,16] P. Lukin,[4,52] M. Masuda,[68] D. Matvienko,[4,52] K. Miyabayashi,[46] H. Miyake,[16,12] H. Miyata,[51] R. Mizuk,[24,42] G. B. Mohanty,[63] S. Mohanty,[63,73] A. Moll,[39,64] H. K. Moon,[32] T. Mori,[44] E. Nakano,[53] M. Nakao,[16,12] T. Nanut,[25] M. Nayak,[19] S. Nishida,[16,12] S. Ogawa,[66] H. Ozaki,[16,12] P. Pakhlov,[24,42] G. Pakhlova,[43,24] B. Pal,[7] C. W. Park,[60] T. K. Pedlar,[37] R. Pestotnik,[25] M. Petrič,[25] L. E. Piilonen,[74] J. Rauch,[65] E. Ribežl,[25] M. Ritter,[39] A. Rostomyan,[8] S. Ryu,[58] H. Sahoo,[15] Y. Sakai,[16,12] S. Sandilya,[63] L. Santelj,[16] T. Sanuki,[67] V. Savinov,[56] O. Schneider,[34] G. Schnell,[1,17] C. Schwanda,[22] Y. Seino,[51] K. Senyo,[76] I. S. Seong,[15] M. E. Sevior,[40] V. Shebalin,[4,52] C. P. Shen,[2] T.-A. Shibata,[70] J.-G. Shiu,[49] F. Simon,[39,64] Y.-S. Sohn,[77] M. Starič,[25] J. Stypula,[50] M. Sumihama,[11] K. Sumisawa,[16,12] T. Sumiyoshi,[71] U. Tamponi,[23,72] K. Tanida,[58] Y. Teramoto,[53] T. Uglov,[24,43] Y. Unno,[14] S. Uno,[16,12] Y. Usov,[4,52] C. Van Hulse,[1] P. Vanhoefer,[39] G. Varner,[15] V. Vorobyev,[4,52] A. Vossen,[20] M. N. Wagner,[10] C. H. Wang,[48] P. Wang,[21] M. Watanabe,[51] Y. Watanabe,[26] K. M. Williams,[74] E. Won,[32] J. Yamaoka,[54] S. Yashchenko,[8] J. Yelton,[9] Y. Yusa,[51] Z. P. Zhang,[57] V. Zhilich,[4,52] V. Zhulanov,[4,52] and A. Zupanc[25]

(The Belle Collaboration)

[1] *University of the Basque Country UPV/EHU, 48080 Bilbao*

[2] *Beihang University, Beijing 100191*

[3] *University of Bonn, 53115 Bonn*

[4] *Budker Institute of Nuclear Physics SB RAS, Novosibirsk 630090*

[5] *Faculty of Mathematics and Physics, Charles University, 121 16 Prague*

[6] *Chonnam National University, Kwangju 660-701*

[7] *University of Cincinnati, Cincinnati, Ohio 45221*

[8] *Deutsches Elektronen–Synchrotron, 22607 Hamburg*

[9] *University of Florida, Gainesville, Florida 32611*

[10] *Justus-Liebig-Universität Gießen, 35392 Gießen*

[11] *Gifu University, Gifu 501-1193*

[12] *SOKENDAI (The Graduate University for Advanced Studies), Hayama 240-0193*

[13] *Gyeongsang National University, Chinju 660-701*

[14] *Hanyang University, Seoul 133-791*

[15] *University of Hawaii, Honolulu, Hawaii 96822*

[16] *High Energy Accelerator Research Organization (KEK), Tsukuba 305-0801*

[17] *IKERBASQUE, Basque Foundation for Science, 48013 Bilbao*

[18] *Indian Institute of Technology Guwahati, Assam 781039*

[19] *Indian Institute of Technology Madras, Chennai 600036*

[20] *Indiana University, Bloomington, Indiana 47408*

[21] *Institute of High Energy Physics,*
Chinese Academy of Sciences, Beijing 100049

[22] *Institute of High Energy Physics, Vienna 1050*

[23] *INFN - Sezione di Torino, 10125 Torino*

[24] *Institute for Theoretical and Experimental Physics, Moscow 117218*

[25] *J. Stefan Institute, 1000 Ljubljana*

[26] *Kanagawa University, Yokohama 221-8686*

[27] *Institut für Experimentelle Kernphysik,*
Karlsruher Institut für Technologie, 76131 Karlsruhe

[28] *Kennesaw State University, Kennesaw GA 30144*

[29] *King Abdulaziz City for Science and Technology, Riyadh 11442*

[30]*Department of Physics, Faculty of Science,*
King Abdulaziz University, Jeddah 21589
[31]*Korea Institute of Science and Technology Information, Daejeon 305-806*
[32]*Korea University, Seoul 136-713*
[33]*Kyungpook National University, Daegu 702-701*
[34]*École Polytechnique Fédérale de Lausanne (EPFL), Lausanne 1015*
[35]*Faculty of Mathematics and Physics,*
University of Ljubljana, 1000 Ljubljana
[36]*Ludwig Maximilians University, 80539 Munich*
[37]*Luther College, Decorah, Iowa 52101*
[38]*University of Maribor, 2000 Maribor*
[39]*Max-Planck-Institut für Physik, 80805 München*
[40]*School of Physics, University of Melbourne, Victoria 3010*
[41]*Middle East Technical University, 06531 Ankara*
[42]*Moscow Physical Engineering Institute, Moscow 115409*
[43]*Moscow Institute of Physics and Technology, Moscow Region 141700*
[44]*Graduate School of Science, Nagoya University, Nagoya 464-8602*
[45]*Kobayashi-Maskawa Institute, Nagoya University, Nagoya 464-8602*
[46]*Nara Women's University, Nara 630-8506*
[47]*National Central University, Chung-li 32054*
[48]*National United University, Miao Li 36003*
[49]*Department of Physics, National Taiwan University, Taipei 10617*
[50]*H. Niewodniczanski Institute of Nuclear Physics, Krakow 31-342*
[51]*Niigata University, Niigata 950-2181*
[52]*Novosibirsk State University, Novosibirsk 630090*
[53]*Osaka City University, Osaka 558-8585*
[54]*Pacific Northwest National Laboratory, Richland, Washington 99352*
[55]*Peking University, Beijing 100871*
[56]*University of Pittsburgh, Pittsburgh, Pennsylvania 15260*
[57]*University of Science and Technology of China, Hefei 230026*
[58]*Seoul National University, Seoul 151-742*
[59]*Soongsil University, Seoul 156-743*

[60] *Sungkyunkwan University, Suwon 440-746*

[61] *School of Physics, University of Sydney, NSW 2006*

[62] *Department of Physics, Faculty of Science, University of Tabuk, Tabuk 71451*

[63] *Tata Institute of Fundamental Research, Mumbai 400005*

[64] *Excellence Cluster Universe, Technische Universität München, 85748 Garching*

[65] *Department of Physics, Technische Universität München, 85748 Garching*

[66] *Toho University, Funabashi 274-8510*

[67] *Tohoku University, Sendai 980-8578*

[68] *Earthquake Research Institute, University of Tokyo, Tokyo 113-0032*

[69] *Department of Physics, University of Tokyo, Tokyo 113-0033*

[70] *Tokyo Institute of Technology, Tokyo 152-8550*

[71] *Tokyo Metropolitan University, Tokyo 192-0397*

[72] *University of Torino, 10124 Torino*

[73] *Utkal University, Bhubaneswar 751004*

[74] *CNP, Virginia Polytechnic Institute and State University, Blacksburg, Virginia 24061*

[75] *Wayne State University, Detroit, Michigan 48202*

[76] *Yamagata University, Yamagata 990-8560*

[77] *Yonsei University, Seoul 120-749*

Abstract

We report the first observation of the decays $B^0 \to p\bar{\Lambda}D^{(*)-}$. The data sample of 711 fb^{-1} used in this analysis corresponds to 772 million $B\bar{B}$ pairs, collected at the $\Upsilon(4S)$ resonance by the Belle detector at the KEKB asymmetric-energy e^+e^- collider. We observe 19.8σ and 10.8σ excesses of events for the two decay modes and measure the branching fractions of $B^0 \to p\bar{\Lambda}D^-$ and $B^0 \to p\bar{\Lambda}D^{*-}$ to be $(25.1 \pm 2.6 \pm 3.5) \times 10^{-6}$ and $(33.6 \pm 6.3 \pm 4.4) \times 10^{-6}$, respectively, where the first uncertainties are statistical and the second are systematic. These results are not compatible with the predictions based on the generalized factorization approach. In addition, a threshold enhancement in the di-baryon ($p\bar{\Lambda}$) system is observed, consistent with that observed in similar B decays.

PACS numbers: 13.25.Hw, 11.30.Er, 12.15.Hh

In the years since the ARGUS and CLEO collaboration first observed baryonic B decays [1, 2], many three-body baryonic B decays ($B \to \mathbf{B}\bar{\mathbf{B}}'\mathbf{M}$) have been found [3–7], where $\mathbf{B}\bar{\mathbf{B}}'$ denotes a baryon-antibaryon system and $\mathbf{M}$ stands for a meson. Although the general pattern of these decays can be understood as the interplay between the short-distance weak interaction and the long-distance strong interaction [8], theories still have difficulties adjusting for various details such as the angular correlation between the energetic outgoing meson and one specific baryon ($\mathbf{B}$) in the di-baryon system [7, 9–11].

A popular theoretical approach used to investigate the three-body baryonic decays is generalized factorization. This method smears the correlation between the weak decay and the fragmentation and allows $B \to \mathbf{B}\bar{\mathbf{B}}'\mathbf{M_c}$ decays (with $\mathbf{M}_c$ denoting a charmed meson) to be categorized into three types: current type, where the $\mathbf{B}\bar{\mathbf{B}}'$ pair is formed by an external W with other quarks; transition type, where the W is internal and forms $\mathbf{BM_c}$; and hybrid (current+transition) type [12]. The $B^0 \to p\bar{\Lambda}D^{(*)-}$ [13] decay belongs to the first type whereas its corresponding charged mode, $B^+ \to p\bar{\Lambda}\bar{D}^{(*)0}$, is of the last type. Using this approach, Ref. [12] predicts the branching fractions

$$\begin{aligned}
\mathcal{B}(B^0 \to p\bar{\Lambda}D^-) &= (3.4 \pm 0.2) \times 10^{-6}, \\
\mathcal{B}(B^0 \to p\bar{\Lambda}D^{*-}) &= (11.9 \pm 0.5) \times 10^{-6}, \\
\mathcal{B}(B^+ \to p\bar{\Lambda}\bar{D}^0) &= (11.4 \pm 2.6) \times 10^{-6}, \\
\mathcal{B}(B^+ \to p\bar{\Lambda}\bar{D}^{*0}) &= (32.3 \pm 3.2) \times 10^{-6}.
\end{aligned} \tag{1}$$

There are two salient features of the predicted results. First, the ratios of the branching fractions of the decays into D^* to the analogous decays into D are $\approx 3:1$. Secondly, the branching fraction of the hybrid-type decay is also ≈ 3 times larger than the corresponding current-type decay. The measured branching fraction for $B^+ \to p\bar{\Lambda}\bar{D}^0$ is consistent with the theoretical calculation based on the factorization approach [12, 14].

In most $B \to \mathbf{B}\bar{\mathbf{B}}'\mathbf{M}$ decay studies, the final-state di-baryon system is observed to favor a mass near threshold [3, 15–17]. While this "threshold enhancement effect" is intuitively understood in terms of the factorization approach, such enhancements are not seen in $B^+ \to p\bar{\Lambda}J/\psi$ nor $B^+ \to \Lambda_c^+\Lambda_c^-K^+$ [18, 19]. More intriguingly, the factorization approach fails to provide a satisfactory explanation for the $\mathbf{M}$–p angular correlations in $B^- \to p\bar{p}K^-$, $B^0 \to p\bar{\Lambda}\pi^-$, and $B^- \to p\bar{p}D^-$ [7, 9–11]. A striking difference between the non-zero angular asymmetries of $B^- \to p\bar{p}D^{*-}$ and $B^- \to p\bar{p}D^-$ was also reported in Ref. [5, 12], for which

a theoretical explanation was attempted in Ref. [20]. A study of pure current-type decays like $B^0 \to p\bar{\Lambda}D^{(*)-}$ is useful to shed more light on the afore mentioned phenomena. In this paper, we report the first observation of $B^0 \to p\bar{\Lambda}D^{(*)-}$ decays using data from the Belle experiment.

The data sample used in this study corresponds to an integrated luminosity of 711 fb^{-1} or 772×10^6 $B\bar{B}$ pairs produced at the $\Upsilon(4S)$ resonance. The Belle detector is located at the interaction point (IP) of the KEKB asymmetric-energy e^+ (3.5 GeV) e^- (8 GeV) collider [21, 22]. It is a large-solid-angle spectrometer comprising six specialized sub-detectors: the Silicon Vertex Detector (SVD), the 50-layer Central Drift Chamber (CDC), the Aerogel Cherenkov Counter (ACC), the Time-Of-Flight scintillation counter (TOF), the electromagnetic calorimeter, and the K_L and muon detector (KLM). A superconducting solenoid surrounding all but the KLM produces a 1.5 T magnetic field [23, 24].

The final-state charged particles, $\pi^{\pm}$, $K^{\pm}$ and $p^{(-)}$, are selected using the likelihood information from the combined tracking (SVD, CDC) and charged-hadron identification (CDC, ACC, TOF) systems [25]. The $B^0 \to p\bar{\Lambda}D^{(*)-}$ signals are reconstructed through the subdecays $D^- \to K^+\pi^-\pi^-$, $D^{*-} \to \bar{D}^0\pi^-$, $\bar{D}^0 \to K^+\pi^-$, and $\bar{\Lambda} \to \bar{p}\pi^+$. The distance of closest approach to the IP by each charged track is required to be less than 3.0 cm along the positron beam (z axis) and 0.3 cm in the transverse plane.The pion and kaon identification efficiencies are in the range of 85–95% while the probability of misidentifying one as the other is 10–20%, both depending on the momentum. The proton identification efficiency is 90–95% for the typical momenta in this study, and the probability of misidentifying a proton as a pion (kaon) is less than 5% (10%). The candidate $\bar{\Lambda}$ is required to have a displaced vertex that is consistent with a long-lived particle originating from the IP and an invariant mass between 1.102 and 1.130 GeV/c^2. The particle-identification criterion is omitted for the daughter pion in the $\bar{\Lambda}$ reconstruction due to the low background rate. For a $\bar{D}^0$, we require the reconstructed invariant mass to lie between 1.72 and 2.02 GeV/c^2. For D^- and D^{*-}, we require $|M_{D^-} - 1870\ \mathrm{MeV}/c^2| < 10\ \mathrm{MeV}/c^2$, $|M_{D^{*-}} - 2010\ \mathrm{MeV}/c^2| < 150\ \mathrm{MeV}/c^2$, and $|M_{D^{*-}} - M_{\bar{D}^0} - 145\ \mathrm{MeV}/c^2| < 9\ \mathrm{MeV}/c^2$, where $M_{D^{(*)-}}$ and $M_{\bar{D}^0}$ are the reconstructed masses of $D^{(*)-}$ and $\bar{D}^0$, respectively.

We identify the signals using two kinematic variables: the energy difference (ΔE) and

the beam-energy-constrained mass ($M_{\rm bc}$),

$$\begin{aligned} \Delta E &= E_B - E_{\rm beam} \\ M_{\rm bc} &= \sqrt{E^2_{\rm beam} - p^2_B c^2}/c^2, \end{aligned} \tag{2}$$

where E_B and p_B are the energy and momentum of the B meson and $E_{\rm beam}$ is the beam energy, all measured in the $\Upsilon(4S)$ center-of-mass (CM) frame.

We optimize all selection criteria using Monte Carlo (MC) event samples before examining the data. These samples, both for signal and background, are generated using EvtGen [26] and later processed with a GEANT3-based detector simulation program that provides the detector-level information [27].

Using the generated MC samples, the fit region is defined as -0.1 GeV $< \Delta E < 0.3$ GeV and 5.22 GeV/$c^2 < M_{\rm bc} <$ 5.30 GeV/c^2 while the signal region is defined as $|\Delta E| < 0.05$ GeV and 5.27 GeV/$c^2 < M_{\rm bc} <$ 5.29 GeV/c^2.

Two major sources contribute as background: $e^+e^- \to q\bar{q}$ ($q = u,\ d,\ s,\ c$) production, also known as the continuum background, and other $b \to c$ dominated B meson decays, labeled generically as B decays in this paper.

To suppress the continuum background, we use the difference between its jet-like topology and the spherical B-decay topology. We calculate the distributions of 23 modified Fox-Wolfram moments from the final-state particle momenta given by the signal and background MC [28, 29]. A Fisher discriminant that enhances the signal and background separation with a weighted linear combination of the moments is then calculated [30]. We augment the obtained probability density functions (PDFs) of the Fisher discriminant for the signal and background with two more variables to form the signal (background) likelihood $\mathcal{L}_{\rm S(B)}$: the axial distance (Δz) between the vertices of the candidate B and the remaining final-state particles — presumably from the other B — and the cosine of the polar angle of the B momentum ($\cos\theta_B$) in the CM frame. The PDFs used for the modified Fox-Wolfram moments, Δz, and $\cos\theta_B$ are bifurcated Gaussian functions, the sums of three Gaussian functions, and second-order polynomials, respectively.

To suppress the background, we optimize the selection criteria for $[\mathcal{L}_{\rm S}/(\mathcal{L}_{\rm S}+\mathcal{L}_{\rm B})]_{D(D^*)} < \alpha_{D(D^*)}$, $|M_{D^-} - 1870$ MeV/$c^2| < \beta_D$ MeV/c^2, and $|M_{D^{*-}} - M_{\bar{D}^0} - 145$ MeV/$c^2| < \beta_{D^*}$ MeV/c^2 simultaneously and obtain $\alpha_D = 0.53$, $\alpha_{D^*} = 0.40$, $\beta_D = 10$, and $\beta_{D^*} = 9$. The β selections correspond to $\pm 2.4\sigma$ and $\pm 12.4\sigma$ selections around the nominal $M_{D^{*-}}$ and

$M_{D^{*-}} - M_{\bar{D}^0}$. This procedure maximizes the figure of merit, $N_{\rm S}/\sqrt{N_{\rm S}+N_{\rm B}}$, where $N_{\rm S}$ and $N_{\rm B}$ are the expected yields of signal and background, respectively, in the signal region. We use the theoretical expectations in Eq. (1) to obtain $N_{\rm S}$ and normalize the $q\bar{q}$ and generic B MC samples to the integrated luminosity to obtain $N_{\rm B}$. After applying all the selection criteria, the fractions of events with multiple signal candidates are found to be 3.5% and 5.6% in the D and D^* modes, respectively. To ensure that no event has multiple entries in the fit region, we retain the B candidate with the smallest vertex-fit χ^2 in each event, where the vertex-fit is performed using all charged tracks from the B candidate except those from $\bar{\Lambda}$.

We model the signal ΔE distribution with the sum of three Gaussian functions; and the $M_{\rm bc}$ distribution with the sum of two Gaussian functions. We model the background ΔE shape with a second-order polynomial; and the $M_{\rm bc}$ shape with an ARGUS function [31]. We determine the PDF shapes with MC samples and calibrate the means and widths of the signal PDFs using a large control sample of $B^0 \to \pi^+ K^0_{\rm S} D^{(*)-}$ decays from the data. The signal yields are extracted separately from eight di-baryon ($p\bar{\Lambda}$) invariant mass bins, in the ranges of 2.05–3.41 GeV/c^2 for the D mode and 2.05–3.30 GeV/c^2 for the D^* mode. We obtain the signal using a two-dimensional extended unbinned maximum likelihood fit in ΔE and $M_{\rm bc}$.

Figure 1 illustrates the fit results of the lowest and highest $p\bar{\Lambda}$ mass bins for the D and D^* modes. We observe clear signal peaks with very low background in the lowest $M_{p\bar{\Lambda}}$ bin, indicating an enhancement near threshold. As the efficiency is dependent on $M_{p\bar{\Lambda}}$, Table I lists the efficiencies and fitted yields in all mass bins for the two modes. Note that the efficiencies shown do not include the sub-decay branching fractions.

Assuming that the branching fractions of $\Upsilon(4S)$ decaying to the charged and neutral $B\bar{B}$ pairs are equal, we use the efficiency and fitted yield in each mass bin to calculate the differential branching fraction and integrate over the entire mass range to obtain the branching fraction $\mathcal{B} = (\sum_i N_i/\epsilon_i)/(\prod \mathcal{B}_{\rm subdecay} \times N_{B\bar{B}} \times C_{\rm PID})$, where i is the mass bin number, N_i and ϵ_i are the bin-dependent fitted yield and selection efficiency, respectively, $\mathcal{B}_{\rm subdecay}$ and $N_{B\bar{B}}$ are the sub-decay branching fraction and the number of $B\bar{B}$ pairs, respectively, and $C_{\rm PID}$ is the charged-particle identification efficiency correction between MC and data (0.92 for the D mode and 0.85 for the D^* mode). Figure 2 shows the results, where both modes have visible peaks near threshold. The data are fit with an empirical threshold yield, $m^a \times e^{(bm+cm^2+dm^3)}$,

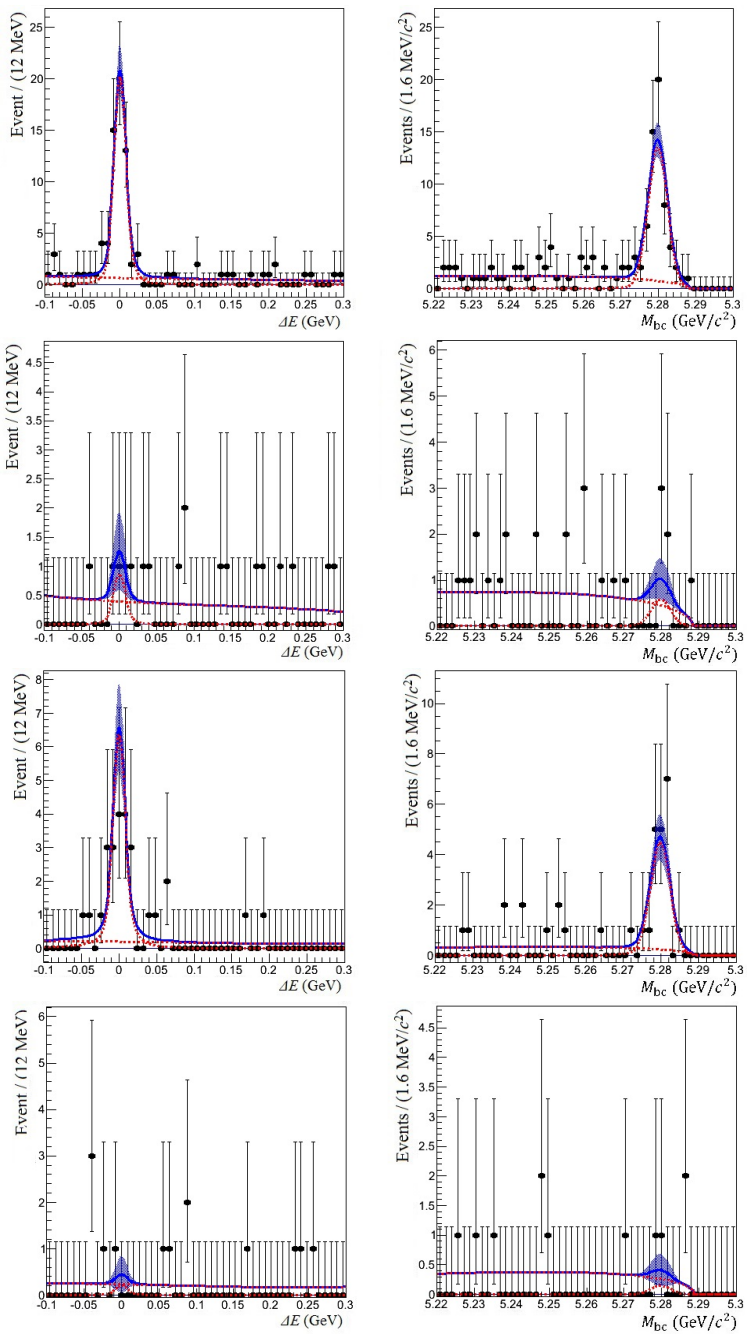

FIG. 1. Projections of typical ΔE-$M_{\rm bc}$ fits to data for events in the signal region of the orthogonal variable. The peaking and flat red dotted lines represent the signal and background components; the blue solid lines with the dotted areas represent the combined PDFs with their 1σ uncertainty bands. The top (bottom) four panels from top to bottom show the fits in the lowest and highest $M_{p\bar{\Lambda}}$ bin in the D (D^*) mode.

vs. the mass excess $m = M_{p\bar{\Lambda}} - M_{\bar{\Lambda}} - M_p$ by varying a, b, c, and d. The obtained branching

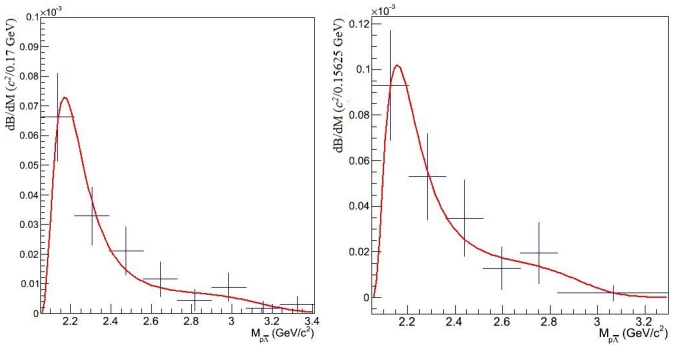

FIG. 2. Differential branching fractions of the D (left) and D^* (right) modes in $M_{p\bar{\Lambda}}$. Fit curves are based on an empirical threshold function (see text).

fractions are:

$$\begin{aligned} \mathcal{B}(B^0 \to p\bar{\Lambda}D^-) &= (25.1 \pm 2.6 \pm 3.5) \times 10^{-6},\ 19.8\sigma, \\ \mathcal{B}(B^0 \to p\bar{\Lambda}D^{*-}) &= (33.6 \pm 6.3 \pm 4.4) \times 10^{-6},\ 10.8\sigma, \end{aligned} \tag{3}$$

where the quoted uncertainties are statistical and systematic (described later), respectively, and the significance is estimated by the Z-score of the p-value for $\chi^2 = 2\sum_i \ln(L_{\max,i}/L_{0,i})$ with 8 or 6 degrees of freedom representing the number of bins. $L_{\max}$ and L_0 are the likelihood values with and without the signal component in the fit, respectively, and i is

TABLE I. The fitted signal yield and efficiency in each $M_{p\bar{\Lambda}}$ bin. To obtain a stable fit, we combine the last three bins in the D^* mode into the sixth bin.

$M_{p\bar{\Lambda}}$	D mode		$M_{p\bar{\Lambda}}$	D^* mode	
(GeV/c^2)	Yield	Eff.(%)	(GeV/c^2)	Yield	Eff.(%)
2.05–2.22	57 ± 8	12.2 ± 0.0	2.05–2.21	19 ± 5	12.2 ± 0.0
2.22–2.39	24 ± 5	10.5 ± 0.0	2.21–2.36	9 ± 3	10.2 ± 0.0
2.39–2.56	14 ± 4	9.5 ± 0.1	2.36–2.52	5 ± 3	8.7 ± 0.0
2.56–2.73	8 ± 3	9.8 ± 0.1	2.52–2.68	2 ± 1	8.4 ± 0.1
2.73–2.90	3 ± 2	10.4 ± 0.1	2.68–2.83	3 ± 2	7.6 ± 0.1
2.90–3.07	7 ± 3	10.9 ± 0.2	2.83–3.30	1 ± 1	6.3 ± 0.1
3.07–3.24	1 ± 2	10.8 ± 0.3			
3.24–3.41	2 ± 2	11.4 ± 0.7			
Total	117 ± 12			39 ± 7	

again the mass bin index. The measured branching fractions are clearly incompatible with the theoretical predictions for both the D and D^* modes [12]. This indicates that the model parameters used in the calculation need to be revised and, perhaps, some modification of the theoretical framework is required.

To extract the decay angular distributions, we divide $\cos\theta_{pD^{(*)}}$ into eight bins, where $\theta_{pD^{(*)}}$ is defined as the angle between the proton and meson directions in the $p\bar{\Lambda}$ rest frame. We follow the same procedure to determine the differential branching fractions in $\cos\theta_{pD^{(*)}}$ as in determining those in $M_{p\bar{\Lambda}}$. Table II lists the fitted signal yields and efficiencies in the $\cos\theta_{pD^{(*)}}$ bins; Fig. 3 shows the differential branching fractions. The efficiency is determined with the MC sample, including the threshold enhancement effect as observed in the data.

We define the angular asymmetry $A_\theta = \frac{\mathcal{B}_+ - \mathcal{B}_-}{\mathcal{B}_+ + \mathcal{B}_-}$, where $\mathcal{B}_{+(-)}$ represents the branching fraction of positive (negative) cosine value. The results are

$$\begin{aligned} A_\theta(B^0 \to p\bar{\Lambda}D^-) &= -0.08 \pm 0.10, \\ A_\theta(B^0 \to p\bar{\Lambda}D^{*-}) &= +0.55 \pm 0.17, \end{aligned} \tag{4}$$

where the uncertainty is purely statistical since the correlated systematic uncertainties cancel in the A_θ calculation. The angular distributions of the D and D^* modes appear to have distinct trends, even though they are both categorized as current-type decays. More data are needed to make the result conclusive.

TABLE II. The fitted signal yield and efficiency in each $\cos\theta_{pD^{(*)}}$ bin.

$\cos\theta_{pD^{(*)}}$	D mode		D^* mode	
	Yield	Eff.(%)	Yield	Eff.(%)
-1.00 – -0.75	10 ± 4	9.0	3 ± 2	8.6
-0.75 – -0.50	17 ± 5	10.5	1 ± 1	10.2
-0.50 – -0.25	16 ± 4	11.5	1 ± 1	11.3
-0.25 – -0.00	15 ± 4	12.2	2 ± 2	12.2
$+0.00$ – $+0.25$	19 ± 5	12.8	7 ± 3	12.7
$+0.25$ – $+0.50$	15 ± 4	13.0	7 ± 3	13.0
$+0.50$ – $+0.75$	16 ± 5	12.6	9 ± 3	12.8
$+0.75$ – $+1.00$	7 ± 3	11.5	8 ± 3	11.5

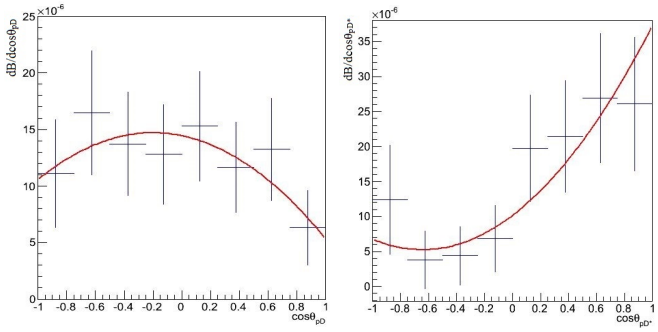

FIG. 3. Differential branching fractions of the D (left) and D^* (right) modes in $\cos\theta_{pD^{(*)}}$. The fit curves are second-order polynomials, as suggested by Ref. [20].

Three major categories of systematic uncertainties are considered: in the signal yield determination, in the efficiency estimation, and in translating the signal yields and efficiencies into the branching fractions. Table III lists all the systematic uncertainties.

We observe a mild peaking background in the $M_{\rm bc}$ fit region due to $B^+ \to p\bar{\Lambda}\bar{D}^{*0}$, plausibly by the replacement of the low-momentum π^0 in $\bar{D}^{*0} \to \bar{D}^0\pi^0$ with an unaffiliated π^- or K^- to reconstruct a D^{*-}. To study its contribution to the uncertainty in the D^* mode, a dedicated MC sample of this background mode is generated. Based on its current branching fraction upper limit [14], we subtract 0.5 events from the extracted signal yield and assign ± 0.5 events as the systematic uncertainty. We have verified that our signal extraction method is robust and see negligible systematic bias in the signal yield when assuming 0.1 to 10 times the theoretical branching fractions (about 1.6 to 160 events) in an MC ensemble test.

For the reconstruction efficiency, we consider the following systematic uncertainties: the signal MC modeling for the threshold enhancement effect using the bound state assumption, charged track reconstruction, charged hadron identification, $\bar{\Lambda}$ reconstruction, background discrimination selections, and the PDF shapes. The modeling uncertainty is estimated by comparing the efficiency calculation based on two different MC samples, one generated assuming p-$\bar{\Lambda}$ bound states and the other with three-body phase-space decays, in each $M_{p\bar{\Lambda}}$ bin. As the result is highly threshold-enhanced, we use the efficiency given by the bound-state model to calculate the branching fractions and take the differences as the systematic uncertainties between the two models. The uncertainty is about 3 (2)% in the D (D^*) mode, depending on the bins. For each charged track except the low-momentum pion in

$D^{*-} \to \bar{D}^0\pi^-$, a 0.35% uncertainty is assigned to take into account the data-MC difference in the charged track reconstruction. For the low-momentum pion, a 2.5% uncertainty is assigned. We use the $\Lambda \to p\pi^-$ and $D^{*+} \to D^0\pi^+$, $D^0 \to K^-\pi^+$ samples to calibrate the MC $(\bar{p})$, $K^\pm$, $\pi^\pm$ identification efficiencies and assign uncertainties. For the $\bar{\Lambda}$ reconstruction, we estimate the uncertainty by considering the data–MC difference of tracks displaced from the IP, the $\bar{\Lambda}$ proper time, and $\bar{\Lambda}$ mass distributions. The uncertainties due to the $\alpha_{D^{(*)}}$ selections are estimated separately with the control sample mode, $B^0 \to \pi^+ K^0_S D^{(*)-}$. We compare the data–MC efficiency differences with or without the α selections, where the non-negligible statistical uncertainties are also included. In both cases, the obtained $\mathcal{B}(B^0 \to \pi^+ K^0_S D^{(*)-})$ is found to be consistent with the world average, indicating overall reliability of our methodology. For the β_D and β_{D^*} selections, we compare the widths of the peaking components in M_{D^-} and $M_{D^{*-}} - M_{\bar{D}^0}$ in the MC and data and quote the differences as the uncertainties. We also relax the shape variables of the signal PDF when fitting the control sample and compare the difference to MC-determined PDF. The resulting difference in the calculated $\mathcal{B}(B^0 \to \pi^+ K^0_S D^{(*)-})$ is negligible.

TABLE III. The systematic uncertainties in the D and D^* modes. The $\approx$ signs indicate the $M_{p\bar{\Lambda}}$ dependence of the uncertainty.

Item	Systematic uncertainty (%)	
	D mode	D^* mode
Yield bias	negligible	1.3 (0.5 evt.)
Modeling	≈ 3	≈ 2
Charged track	2.1	4.3
Charged hadron identification	1.3	1.8
$\bar{\Lambda}$ identification	4.0	4.4
M_{D^-}, $M_{D^{*-}} - M_{\bar{D}^0}$ window	2.0	negligible
$\mathcal{L}_{\rm S}/(\mathcal{L}_{\rm S} + \mathcal{L}_{\rm B})$ requirement	11.5	11.0
PDF shape	negligible	negligible
$N_{B\bar{B}}$	1.4	1.4
Sub-decay $\mathcal{B}$	2.2	1.7
Overall	13.9	13.1

In the translation from signal yields to branching fractions, we consider the uncertainties of $\mathcal{B}_{\rm subdecay}$ and $N_{B\bar{B}}$. The uncertainties of $\mathcal{B}_{\rm subdecay}$ are obtained from Ref. [3]. For $N_{B\bar{B}}$, on- and off- resonance di-lepton events, $e^+e^- \to q\bar{q}$ MC and data difference, primary vertex sideband data, and statistical uncertainty are combined to estimate the uncertainty.

In this paper, we have reported the first observation of the $B^0 \to p\bar{\Lambda}D^-$ and $B^0 \to p\bar{\Lambda}D^{*-}$ decays with branching fractions $(25.1 \pm 2.6 \pm 3.5) \times 10^{-6}$ (19.8σ) and $(33.6 \pm 6.3 \pm 4.4) \times 10^{-6}$ (10.8σ). The threshold enhancement effect observed in $M_{p\bar{\Lambda}}$ is found to be consistent with many other three-body baryonic B decays. The obtained branching fractions disagree with predictions based on the factorization approach, as do the measured ratios of branching fractions, both for the D and D^* modes and for the charged and neutral B modes. We also find potential angular asymmetry in the D^* mode but not in the D mode. Theoretical explanations, as well as confirmation from experiments with sizable data sets, such as LHCb and Belle II, will be needed in the future.

We thank the KEKB group for the excellent operation of the accelerator; the KEK cryogenics group for the efficient operation of the solenoid; and the KEK computer group, the National Institute of Informatics, and the PNNL/EMSL computing group for valuable computing and SINET4 network support. We acknowledge support from the Ministry of Education, Culture, Sports, Science, and Technology (MEXT) of Japan, the Japan Society for the Promotion of Science (JSPS), and the Tau-Lepton Physics Research Center of Nagoya University; the Australian Research Council and the Australian Department of Industry, Innovation, Science and Research; Austrian Science Fund under Grant No. P 22742-N16 and P 26794-N20; the National Natural Science Foundation of China under Contracts No. 10575109, No. 10775142, No. 10875115, No. 11175187, and No. 11475187; the Ministry of Education, Youth and Sports of the Czech Republic under Contract No. LG14034; the Carl Zeiss Foundation, the Deutsche Forschungsgemeinschaft and the VolkswagenStiftung; the Department of Science and Technology of India; the Istituto Nazionale di Fisica Nucleare of Italy; National Research Foundation (NRF) of Korea Grants No. 2011-0029457, No. 2012-0008143, No. 2012R1A1A2008330, No. 2013R1A1A3007772, No. 2014R1A2A2A01005286, No. 2014R1A2A2A01002734, No. 2014R1A1A2006456; the Basic Research Lab program under NRF Grant No. KRF-2011-0020333, No. KRF-2011-0021196, Center for Korean J-PARC Users, No. NRF-2013K1A3A7A06056592; the Brain Korea 21-Plus program and the Global Science Experimental Data Hub Center of the Korea Institute of Science and Technology

Information; the Polish Ministry of Science and Higher Education and the National Science Center; the Ministry of Education and Science of the Russian Federation and the Russian Foundation for Basic Research; the Slovenian Research Agency; the Basque Foundation for Science (IKERBASQUE) and the Euskal Herriko Unibertsitatea (UPV/EHU) under program UFI 11/55 (Spain); the Swiss National Science Foundation; the Ministry of Science and Technology and the Ministry of Education of Taiwan; and the U.S. Department of Energy and the National Science Foundation. This work is supported by a Grant-in-Aid from MEXT for Science Research in a Priority Area ("New Development of Flavor Physics") and from JSPS for Creative Scientific Research ("Evolution of Tau-lepton Physics").

* gixd@hep1.phys.ntu.edu.tw

† mwang@hep1.phys.ntu.edu.tw

[1] H. Albrecht *et al.* (ARGUS Collaboration), Phys. Lett. B **210**, 263 (1988).

[2] G. Crawford *et al.* (CLEO Collaboration), Phys. Rev. D **45**, 752 (1992).

[3] K. A. Olive *et al.* (Particle Data Group), Chin. Phys. C **38**, 090001 (2014).

[4] K. Abe *et al.* (Belle Collaboration), Phys. Rev. Lett. **89**, 151802 (2002).

[5] B. Aubert *et al.* (BaBar Collaboration), Phys. Rev. D **74**, 051101 (2006).

[6] J.-H. Chen *et al.* (Belle Collaboration), Phys. Rev. Lett. **100**, 251801 (2008).

[7] J.-T. Wei *et al.* (Belle Collaboration), Phys. Lett. B **659**, 80 (2008).

[8] M. Suzuki, J. Phys. G **34**, 283 (2007).

[9] M.-Z. Wang *et al.* (Belle Collaboration), Phys. Lett. B **617**, 141 (2005).

[10] M.-Z. Wang *et al.* (Belle Collaboration), Phys. Rev. D **76**, 052004 (2007).

[11] P. del Amo Sanchez *et al.* (BaBar Collaboration), Phys. Rev. D **85**, 092017 (2012).

[12] C. H. Chen *et al.*, Phys. Rev. D. **78**, 054016 (2008).

[13] Hereafter, the inclusion of the charge-conjugate mode is implied.

[14] P. Chen *et al.* (Belle Collaboration), Phys. Rev. D **84**, 071501 (2011).

[15] J. Z. Bai *et al.* (BES Collaboration), Phys. Rev. Lett. **91**, 022001 (2003).

[16] M. Ablikim *et al.* (BES Collaboration), Phys. Rev. Lett. **95**, 262001 (2005).

[17] J. P. Alexander *et al.* (CLEO Collaboration), Phys. Rev. D **82**, 092002 (2010).

[18] Q. L. Xie *et al.* (Belle Collaboration), Phys. Rev. D **72**, 051105 (2005).

[19] N. Gabyshev *et al.* (Belle Collaboration), Phys. Rev. Lett. **97**, 202003 (2006).

[20] C. Q. Geng and Y. K. Hsiao, Phys. Rev. D **74**, 094023 (2006).

[21] S. Kurokawa and E. Kikutani, Nucl. Inst. and Meth. in Phys. Res. sec. A **499**, 1 (2003), and other papers included in this volume.

[22] T. Abe *et al.*, Prog. Theor. Exp. Phys. **03A001** (2013).

[23] A. Abashian *et al.* (Belle Collaboration), Nucl. Inst. and Meth. in Phys. Res. sec. A **479**, 117 (2002).

[24] J. Brodzicka *et al.*, Prog. Theor. Exp. Phys. **04D001** (2012), detector section.

[25] E. Nakano *et al.* (Belle Collaboration), Nucl. Inst. and Meth. in Phys. Res. sec. A **494**, 402 (2002).

[26] D. J. Lange, Nucl. Inst. and Meth. in Phys. Res. A **462**, 152 (2001).

[27] R. Brun *et al.*, CERN Report DD/EE/84-1 (1984).

[28] G. C. Fox and S. Wolfram, Phys. Rev. Lett. **41**, 1581 (1978), the modified moments used in this paper are described in [29].

[29] S. H. Lee *et al.* (Belle Collaboration), Phys. Rev. Lett. **91**, 261801 (2003).

[30] R. A. Fisher, Annals of Eugenics **7**, 179 (1936).

[31] H. Albrecht *et al.* (ARGUS Collaboration), Phys. Lett. B **241**, 278 (1990).